Supporting Information for

Incarceration of one or two phosphate or arsenate species within nanojars, capped nanojars and helicages: helical chirality from two closely-spaced, head-to-head PO_4^{3-} or AsO_4^{3-} ions

Gellert Mezei
Department of Chemistry, Western Michigan University, Kalamazoo, Michigan 49008, USA
E-mail: gellert.mezei@wmich.edu

EXPERIMENTAL DETAILS

Synthesis. Copper hydroxide was freshly prepared by mixing ice-cold aqueous solutions of $Cu(NO_3)_2 \cdot 2.5H_2O$ (902 mg, 3.88 mmol) and NaOH (310 mg, 7.75 mmol) under stirring, followed by filtration under a blanket of N_2 and thorough washing with water, and then with THF. The resulting $Cu(OH)_2$ powder was stirred with pyrazole (264 mg, 3.88 mmol), Bu_4NOH (1 M in H_2O, 730 mg, 0.730 mmol) and H_3PO_4 (85% in H_2O, 28 mg, 0.243 mmol) in 20 mL THF overnight, then the deep blue solution was filtered and evaporated. Yield: 684 mg dark blue powder. The arsenate analog was obtained similarly, using 505 mg Bu_4NOH (1M in H_2O, 0.505 mmol) and 86 mg $Na_2HAsO_4 \cdot 7H_2O$ (0.276 mmol). Yield: 730 mg dark blue powder. Crystals of $(Bu_4N)_2[HXO_4^{2-} \subset \{Cu^{II}(\mu\text{-OH})(\mu\text{-pz})\}_{31}]$ (**1**, X = P; **2**, X = As) were obtained by hexane vapor diffusion into toluene solutions. Crystals of $(Bu_4N)[PO_4^{3-} \subset \{Cu^{II}_{30}(\mu\text{-OH})_{27}(\mu_3\text{-OCH}_3)(\mu\text{-pz})_{30}(CH_3OH)_2\}]$ (**3**) were grown by methanol vapor diffusion into an *n*-butyl acetate solution. Crystals of $(Bu_4N)_2[(XO_4^{3-})_2 \subset \{Cu^{II}_{15}(\mu_3\text{-OH})_2(\mu\text{-OH})_6(\mu\text{-pz})_{18}\}]$ (**4**, X = P; **5**, X = As) were grown from bromobenzene/nitrobenzene (1:1) solutions by hexane vapor diffusion.

Anion binding studies. 500 mg of the product obtained above was dissolved in 10 ml toluene, filtered, then stirred vigorously with 10 ml saturated aqueous $Ba(OH)_2$ solution (~0.16 M, pH 13.5) under an N_2 atmosphere. After five weeks of stirring, no precipitation was observed and the electronic spectrum of the nanojar solution remained unchanged (λ_{max} = 600 nm).

X-RAY CRYSTALLOGRAPHY

X-ray diffraction data were collected at 100 K from a single-crystal mounted atop a glass fiber under Paratone-N oil, with a Bruker SMART APEX II diffractometer using graphite-monochromated Mo-Kα (λ = 0.71073 Å) radiation. Once removed from the mother liquor, all

crystals were extremely sensitive to solvent loss at ambient conditions and were mounted quickly under a cryostream to prevent decomposition. The structures were solved by employing SHELXTL direct methods and refined by full-matrix least squares on F^2, using the APEX2 v2014.9-0 software package (Bruker AXS Inc.: Madison, WI, 2014). All non-H atoms were refined with independent anisotropic displacement parameters, except some of the disordered molecules (see below), to which geometrical restraints (distances) or constraints (phenyl rings as regular hexagons) were applied. C–H hydrogen atoms were placed in idealized positions (except for the disordered atoms) and refined using the riding model. Crystallographic details are summarized in Table S1.

1: $(Bu_4N)_2[HPO_4^{2-}\subset\{Cu^{II}(\mu\text{-}OH)(\mu\text{-}pz)\}_{31}]\cdot(C_6H_5CH_3)_3\cdot(C_6H_{14})_2\cdot(C_6H_{12})$. One complete Bu_4N^+ counterion, two C-atoms of the other Bu_4N^+ counterion, as well as a methylcyclopentane solvent molecule (from the mixture of hexane isomers used for crystal growing), are disordered over two positions (50/50). H-atoms for OH groups and the HPO_4^{2-} ion were not located.

2: $(Bu_4N)_2[HAsO_4^{2-}\subset\{Cu^{II}(\mu\text{-}OH)(\mu\text{-}pz)\}_{31}]\cdot(C_6H_5CH_3)_2\cdot(C_6H_{14})$. The arsenate ion and three pyrazolate rings are disordered over two positions (50/50 and 50/50, 50/50, 67/33, respectively). The Bu_4N^+ counterions, as well as the toluene and hexane solvent molecules are also disordered. The disorder was modeled over two positions (50/50) for all solvent molecules, and for one Bu_4N^+ ion. Only 18 of the 31 OH hydrogens could be located form the residual electron density map.

3: $(Bu_4N)[PO_4^{3-}\subset\{Cu^{II}_{30}(\mu\text{-}OH)_{27}(\mu_3\text{-}OCH_3)(\mu\text{-}pz)_{30}(CH_3OH)_2\}]\cdot(CH_3OH)_8$. The Bu_4N^+ counterion appears slightly disordered (relatively large thermal ellipsoids), but the disorder was not modeled (refined isotropically, without hydrogens). The methanol solvent molecules are severely disordered; the disorder was modeled over two positions (50/50). Methanol OH hydrogens were not located; only 16 of the 27 OH groups of the nanojar could be located from the residual electron density map.

4: $(Bu_4N)_2[(PO_4^{3-})_2\subset\{Cu^{II}_{15}(\mu_3\text{-}OH)_2(\mu\text{-}OH)_6(\mu\text{-}pz)_{18}\}]\cdot(C_6H_5NO_2)_{1.5}\cdot(C_6H_5Br)_{1.5}$. One butyl arm of one of the two Bu_4N^+ counterions is disordered over two positions (50/50). One of the nitrobenzene solvent molecules is disordered with a bromobenzene molecule (50/50). Another bromobenzene molecule is disordered over two positions (50/50).

5: $(Bu_4N)_2[(AsO_4^{3-})_2\subset\{Cu^{II}_{15}(\mu_3\text{-}OH)_2(\mu\text{-}OH)_6(\mu\text{-}pz)_{18}\}]\cdot(C_6H_5NO_2)_2\cdot(C_6H_5Br)_2$. The helicage is located on a special position (two-fold axis passing in-between the two arsenate ions) and is

disordered over two positions (50/50), with a shared $Cu(pz)_2$ unit centered on the two-fold axis. The Bu_4N^+ counterion, nitrobenzene and bromobenzene solvent molecules are also disordered over two positions (50/50). The heavier atoms (copper and arsenic) were refined anisotropically, and all lighter atoms were refined isotropically. No hydrogen atoms were placed.

Table S1. Summary of the crystallographic data.

	GM116·$(C_6H_5CH_3)_3$·$(C_6H_{14})_2$·(C_6H_{12})	**GM119·$(CH_3OH)_8$**	**GM114·$(C_6H_5NO_2)_{1.5}$·$(C_6H_5Br)_{1.5}$**	**GM138·$(C_6H_5CH_3)_2$·(C_6H_{14})**	**GM132·$(C_6H_5NO_2)_2$·$(C_6H_5Br)_2$**
Formula	$C_{164}H_{261}Cu_{31}N_{64}O_{35}P$	$C_{117}H_{196}Cu_{30}N_{61}O_{42}P$	$C_{104}H_{149}Br_{1.5}Cu_{15}N_{39.5}O_{19}P_2$	$C_{145}H_{227}AsCu_{31}N_{64}O_{35}$	$C_{110}H_{154}As_2Br_2Cu_{15}N_{40}O_{20}$
FW	5690.06	5066.51	3391.52	5471.55	3619.48
Crystal system	triclinic	monoclinic	monoclinic	triclinic	monoclinic
Space group	P ī	$P2_1/c$	$P2_1/c$	P ī	C2/c
a/Å	20.4153(9)	19.9142(3)	17.1774(2)	20.4878(3)	17.3262(4)
b/Å	22.910(1)	28.2823(4)	24.4000(3)	22.9195(4)	25.3190(5)
c/Å	25.866(1)	33.9811(5)	33.5490(4)	25.7171(4)	31.9199(7)
α/deg	103.685(3)	90.000	90.000	103.640(1)	90.000
β/deg	94.975(3)	106.132(1)	103.254(1)	95.220(1)	102.256(1)
γ/deg	110.593(3)	90.000	90.000	110.663(1)	90.000
V/Å^3	10809.7(9)	18385.2(5)	13686.8(3)	10777.1(3)	13683.5(5)
Z	2	4	4	2	4
D_{calc}/g cm^{-3}	1.748	1.830	1.646	1.686	1.757
μ/mm^{-1}	3.061	3.478	2.811	3.211	3.418
Reflns collected/unique	206783/38159	296310/37767	197392/24276	354727/38290	107747/12193
Obsd reflns [$I > 2\sigma(I)$]	27784	19734	15790	14010	6231
Data/parameters	38159/2465	37767/2207	24276/1593	38290/21386	12193/817
GOF (on F^2)	1.119	1.014	0.952	1.006	1.005
R(F), R_w(F) [$I > 2\sigma(I)$]	0.1289, 0.3390	0.0844, 0.1837	0.0690, 0.1621	0.0822, 0.1770	0.0815, 0.1893
R(F), R_w(F) [all data]	0.1616, 0.3555	0.1820, 0.2333	0.1182, 0.1901	0.1619, 0.2196	0.1708, 0.2477

Table S2. Summary of the hydrogen bonding data in **1**−**3**.

1		**2**		**3**	
D−H···A	D···A (Å)	D−H···A	D···A (Å)	D−H···A	D···A (Å)
O3 O32	3.04(2)	O7 O32a	2.77(3)	O4 O30	2.769(13)
O4 O32	2.87(2)	O8 O32a	2.59(3)	O25 O30	2.868(14)
O27 O32	2.78(2)	O23 O32a	2.87(2)	O26 O30	2.648(12)
O28 O32	2.88(2)	O24 O32a	3.06(2)	O27 O30	2.922(15)
		O8 O32b	2.96(3)		
		O23 O32b	2.71(2)		
		O24 O32b	2.89(2)		
O1 O33	2.82(2)	O4 O33	3.05(1)	O6 O31	2.675(13)
O8 O33	3.02(2)	O5 O33	2.80(1)	O19 O31	2.876(15)
O24 O33	2.95(2)	O6 O33	3.04(2)	O20 O31	2.665(12)
O25 O33	3.03(2)	O29 O33	2.95(2)	O21 O31	2.795(13)
		O30 O33	2.91(1)		
O23 O34	3.05(3)	O31 O35a	2.91(3)	O34 O12	2.583(13)
		O28 O35b	3.03(2)	O33 O16	2.593(12)
O6 O35	2.77(3)	O2 O34a	3.00(2)	O2 O32	2.749(12)
O7 O35	2.91(3)	O26 O34a	2.81(2)	O22 O32	2.905(13)
O30 O35	3.04(2)	O27 O34a	2.66(2)	O23 O32	2.663(14)
O31 O35	2.84(2)	O2 O34b	2.60(2)	O24 O32	2.833(14)
		O3 O34b	2.85(2)		
		O26 O34b	2.92(2)		
		O27 O34b	2.88 (2)		
O11 O1	2.84(2)	O11 O1	2.88(1)	O10 O1	2.776(13)
O9 O8	2.90(2)	O13 O2	2.77(1)	O12 O2	2.657(16)
O20 O6	2.80(2)	O16 O4	2.86(1)	O14 O3	2.780(14)
O18 O5	2.86(2)	O18 O5	2.80(1)	O16 O4	2.622(12)
O16 O4	2.78(2)	O20 O6	2.90(1)	O18 O5	2.764(15)
O13 O2	2.86(2)	O9 O8	2.77(1)	O8 O6	2.745(13)
O17 O28	2.82(2)	O10 O24	2.77(2)	O7 O19	2.742(14)
O15 O27	2.81(2)	O12 O26	2.77(1)	O9 O21	2.750(13)
O12 O25	2.80(2)	O14 O27	2.80(1)	O11 O22	2.871(12)
O10 O24	2.85(2)	O17 O29	2.84(1)	O13 O24	2.940(12)
O21 O31	2.77(2)	O19 O30	2.85(1)	O15 O25	2.938(12)
O19 O30	2.81(3)	O22 O23	2.75(2)	O17 O27	2.833(17)

Table S3. Summary of the hydrogen bonding data in **4**−**5**.

Compound	D−H···A	D···A (Å)	D−H (Å)	H···A (Å)	D−H−A (°)	Symmetry operator for D
4	O3-H3o O12	2.653(8)	0.83(2)	1.88(5)	153(10)	
	O5-H5o O12	2.649(9)	0.83(2)	1.84(4)	162(11)	
	O7-H7o O12	2.679(8)	0.83(2)	1.89(5)	157(11)	
	O4-H4o O16	2.653(7)	0.83(2)	1.99(7)	136(9)	
	O6-H6o O16	2.712(8)	0.84(2)	1.94(5)	151(10)	
	O8-H8o O16	2.687(8)	0.83(2)	1.90(4)	157(10)	
5	O6a O1a	2.66(2)				2−x, y, 1/2−z
	O7b O1a	2.72(2)				
	O8a O1a	2.681(18)				
	O6b O1b	2.67(2)				2−x, y, 1/2−z
	O7a O1b	2.70(2)				
	O8b O1b	2.671(18)				

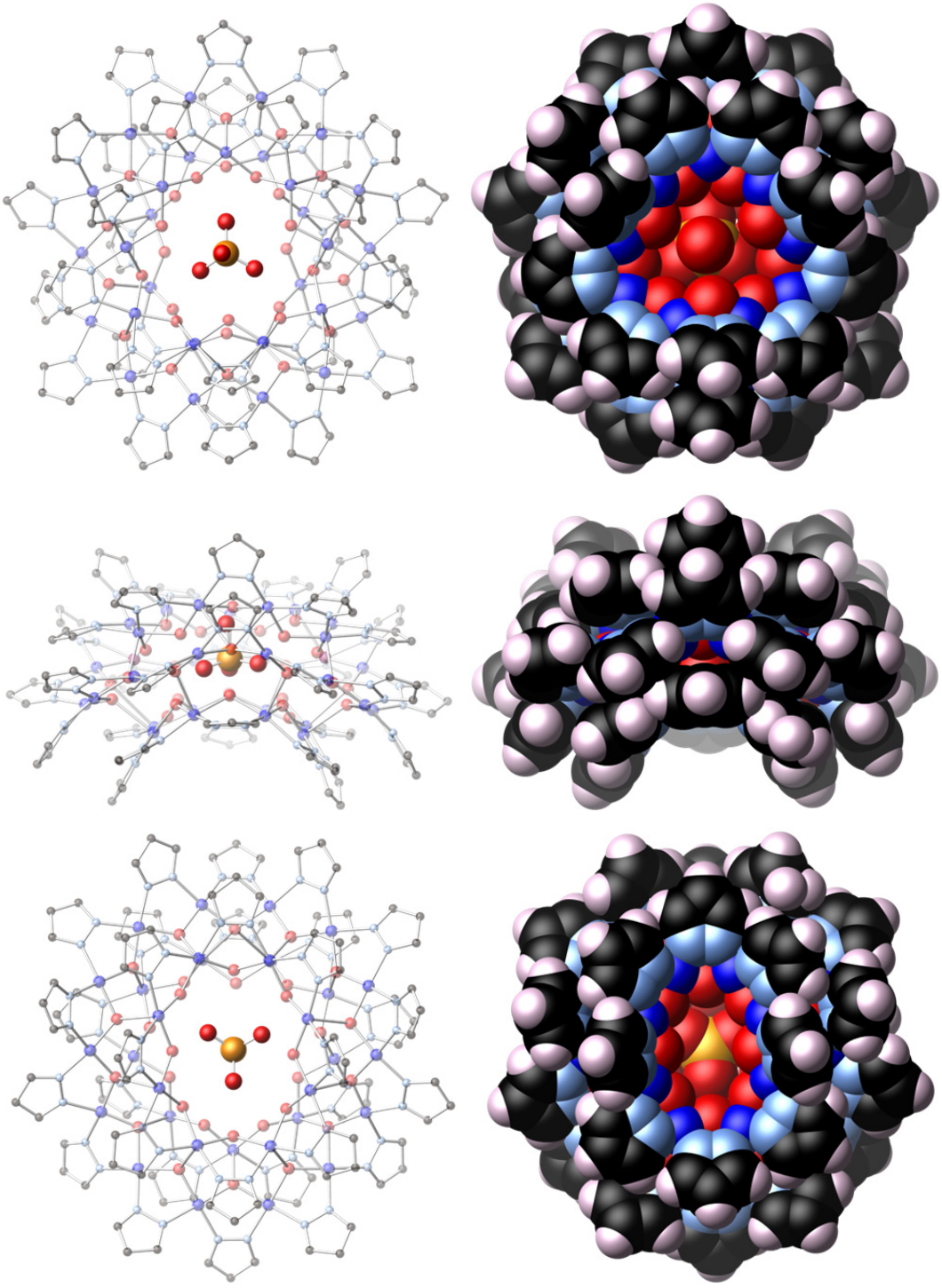

Figure S1. Ball-and-stick (no H-atoms shown) and space filling representations of the crystal structure of **1** (top-, side- and bottom-views).

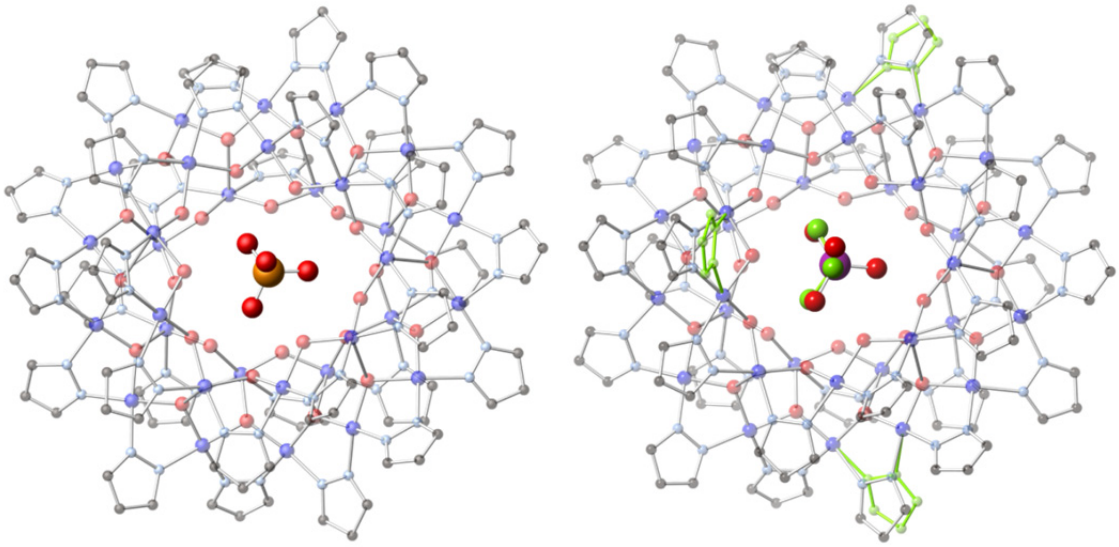

Figure S2. Comparative view of **1** (left) and **2** (right), showing the virtual identity of the two structures, as well as the position of the disordered pyrazole rings and arsenate O-atoms in **2** (in green). The disorder is less severe in **1** and it was not modeled. H-atoms are not shown for clarity. Color code: Cu−dark blue; P−orange; As−purple; O−red; N−light blue; C−black.

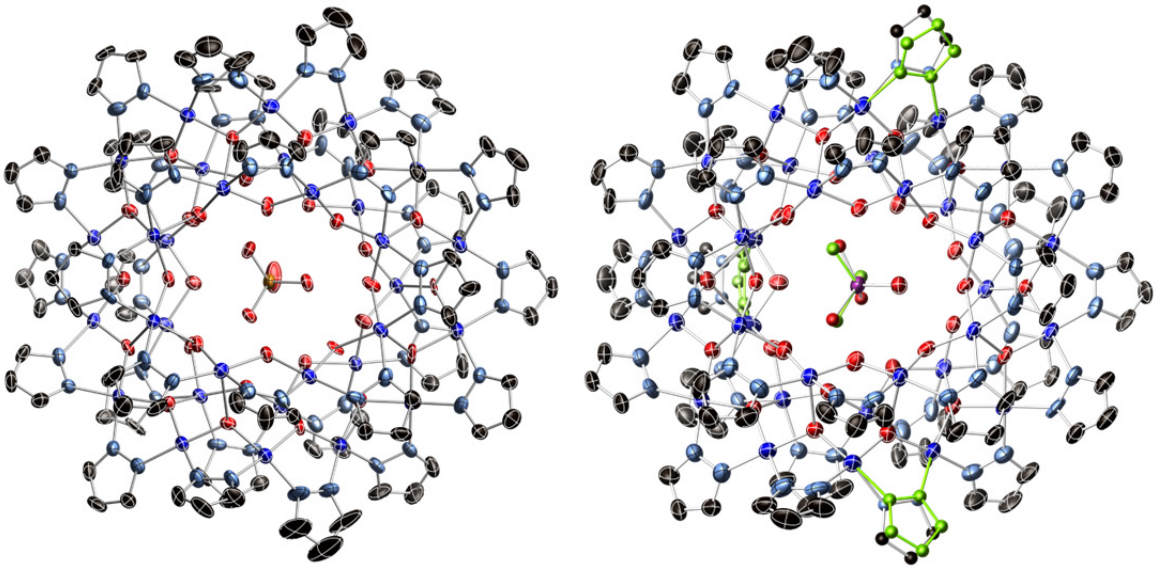

Figure S3. Thermal ellipsoid plots (50% probability) of **1** (left) and **2** (right). H-atoms, counterions and solvent molecules are omitted for clarity. Color code: Cu−dark blue; P−orange; As−purple; O−red; N−light blue; C−black.

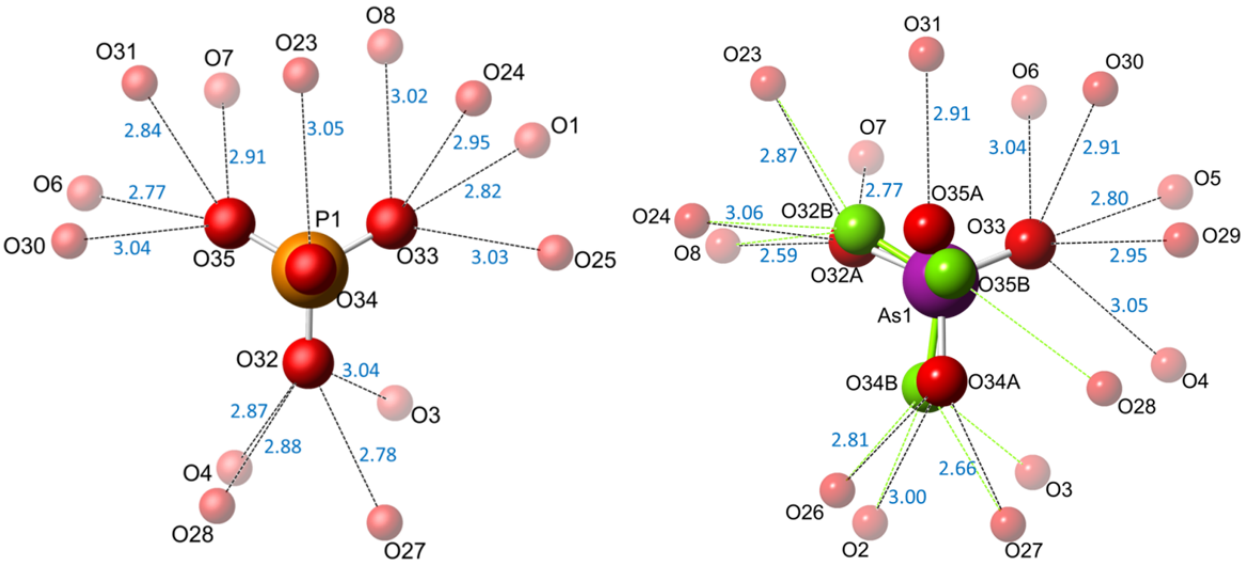

Figure S4. Hydrogen bonding around the HPO_4^{2-} and $HAsO_4^{2-}$ ions in **1** (left) and **2** (right) (O···O distances in Å). The H-atom of the HXO_4^{2-} ions is located on O34 and O35, respectively. Estimated standard deviations, as well as distances for the disordered atoms shown in green, are presented in Table S2.

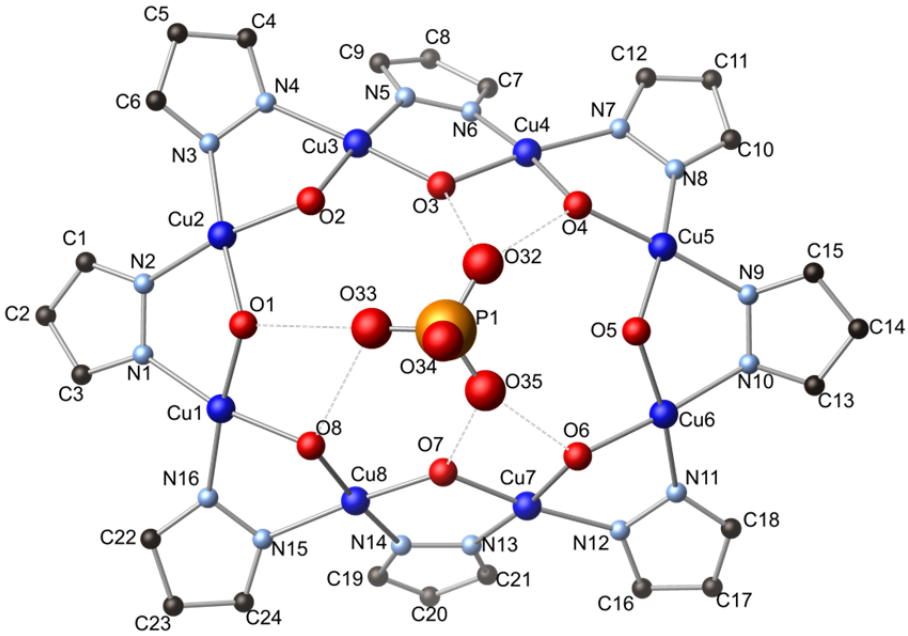

Figure S5. Hydrogen bonding between the HPO_4^{2-} ion and the 8-membered ring in **1** (H-atoms not shown).

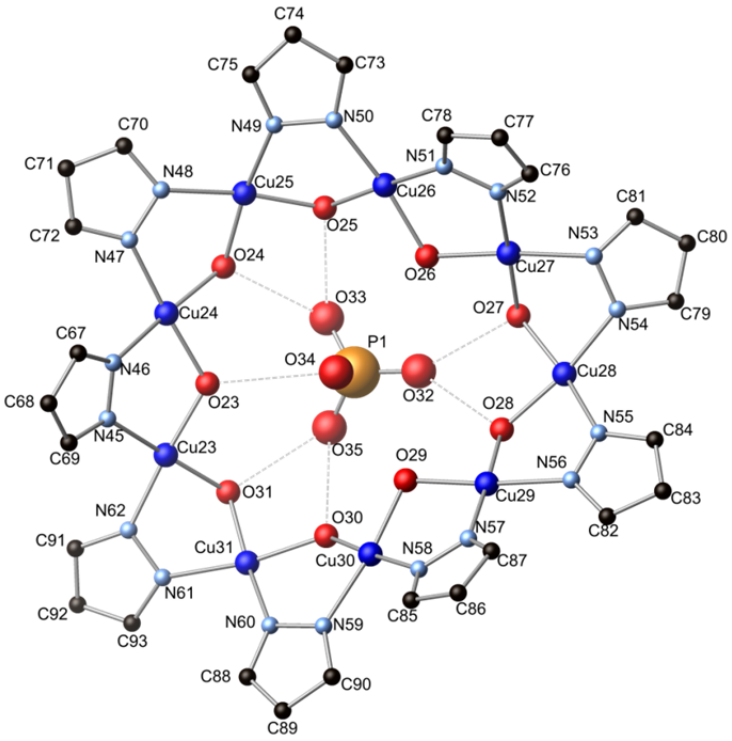

Figure S6. Hydrogen bonding between the HPO_4^{2-} ion and the 9-membered ring in **1** (H-atoms not shown).

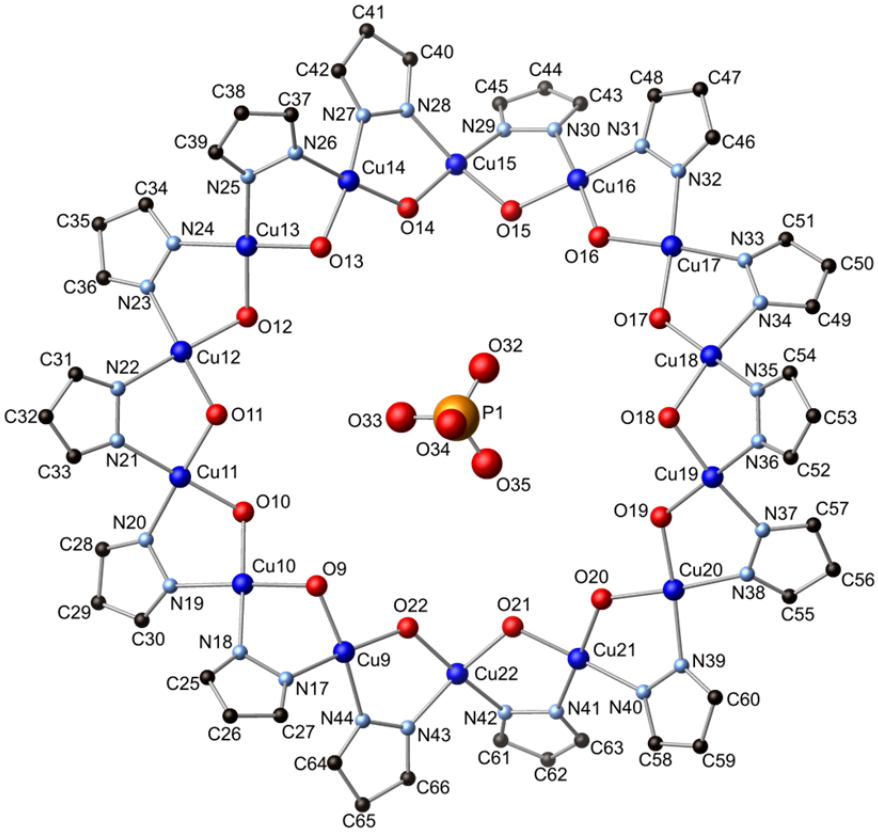

Figure S7. Illustration of the HPO_4^{2-} ion centered in the 14-membered ring in **1** (H-atoms not shown).

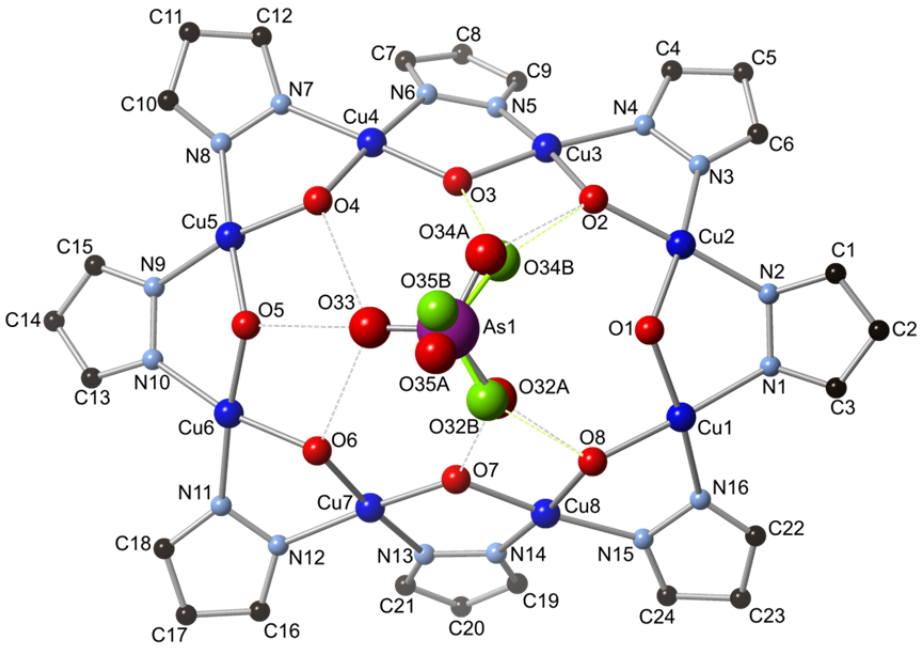

Figure S8. Hydrogen bonding between the $HAsO_4^{2-}$ ion and the 8-membered ring in **2** (H-atoms not shown). Color code: Cu−dark blue; As−purple; O−red; N−light blue; C−black. Disordered arsenate O-atoms are shown in green.

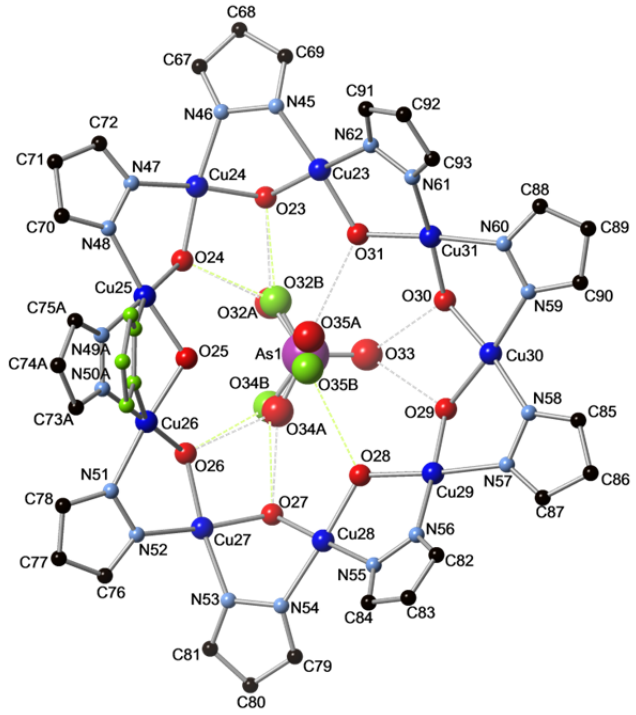

Figure S9. Hydrogen bonding between the $HAsO_4^{2-}$ ion and the 9-membered ring in **2** (H-atoms not shown). Disordered pyrazole rings and arsenate O-atoms are shown in green.

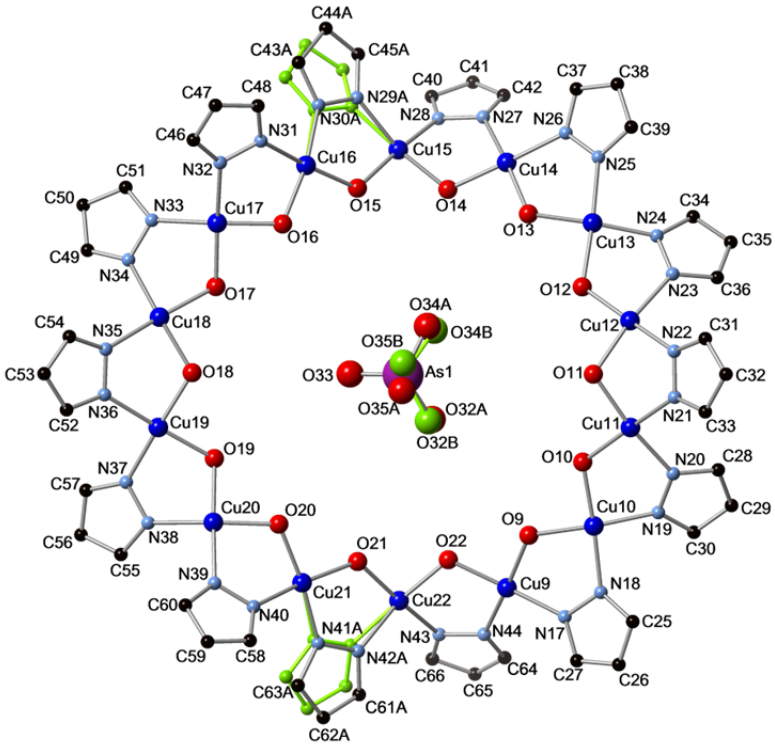

Figure S10. Hydrogen bonding between the $HAsO_4^{2-}$ ion and the 14-membered ring in **2** (H-atoms not shown). Disordered pyrazole rings and arsenate O-atoms are shown in green.

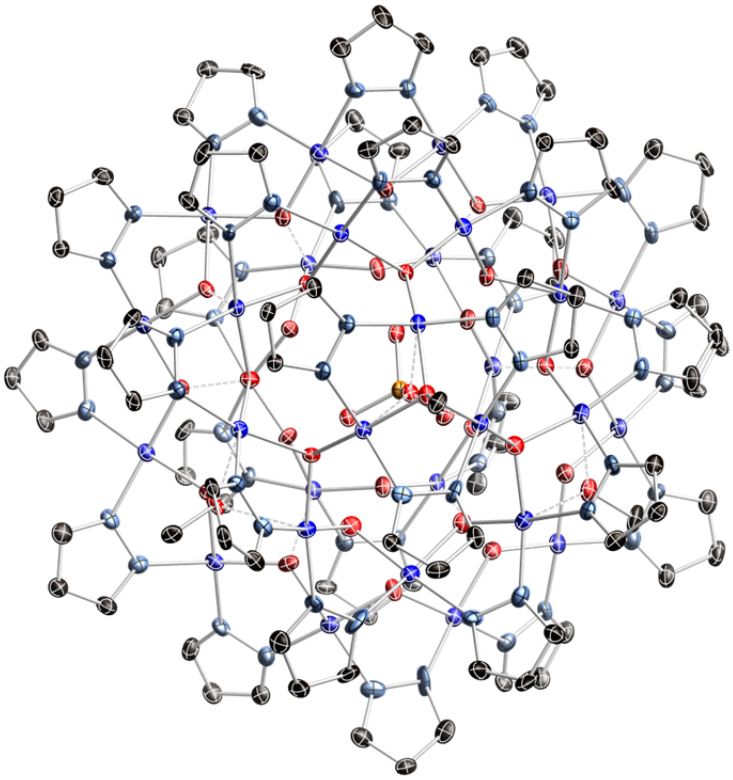

Figure S11. Thermal ellipsoid plot (50% probability) of **3**. H-atoms, counterions and solvent molecules are omitted for clarity. Color code: Cu−dark blue; P−orange; O−red; N−light blue; C−black.

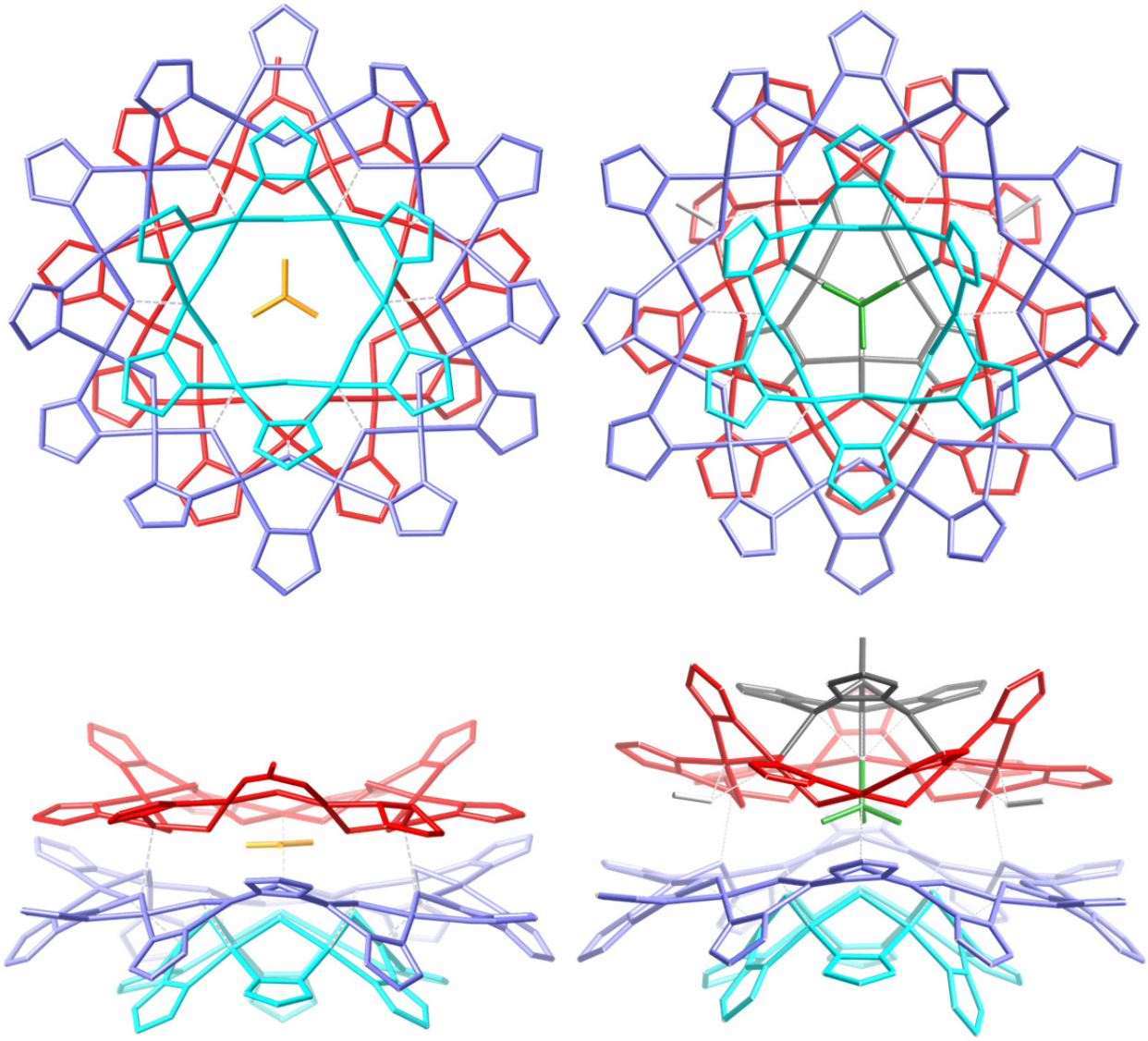

Figure S12. Comparative view of the structures of the Cu6+12+9 nanojars with incarcerated CO_3^{2-} (left, orange; from ref. 13b) and PO_4^{3-} (right, green), showing the different orientation (180° rotation) of the 9-membered ring relative to the 6+12 ring combination (red: 9-membered ring; violet: 12-membered ring; light blue: 6-membered ring; dark grey: trinuclear ring; light grey: methanol; H-atoms not shown; the 9-membered ring in the carbonate-nanojar has one pyrazolate unit substituted by acetate; dashed lines: weak Cu−O bonds).

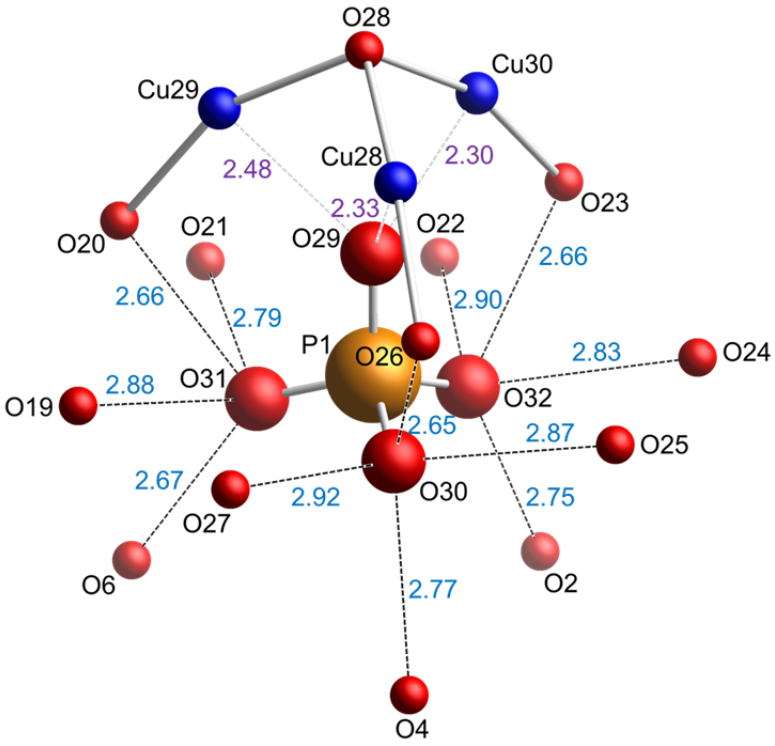

Figure S13. Hydrogen bonding around the PO_4^{3-} ion in **3** (O···O and Cu···O distances in Å). Estimated standard deviations are presented in Table S2.

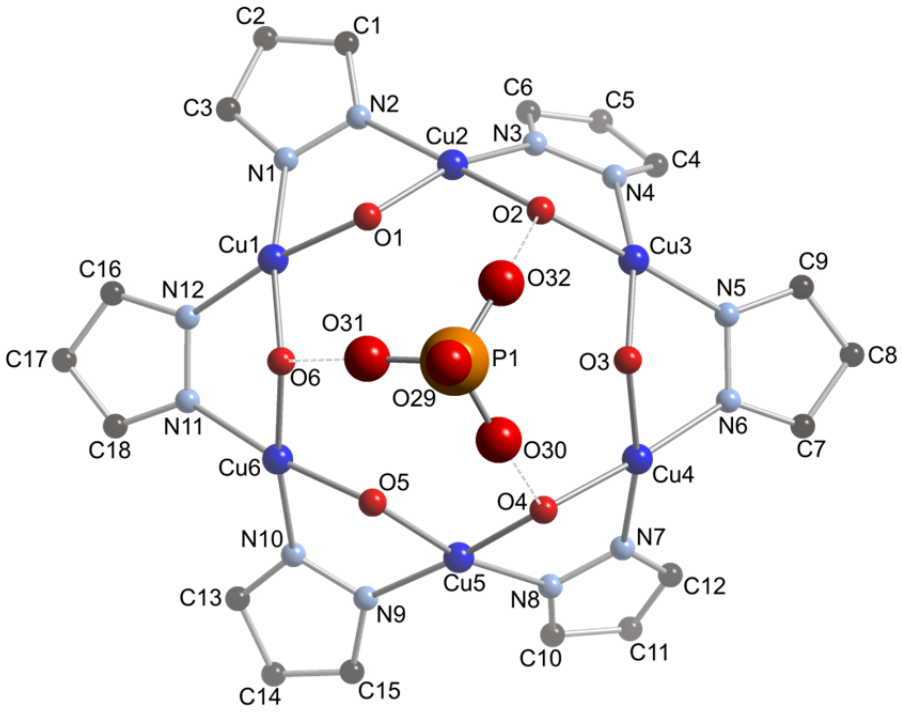

Figure S14. Hydrogen bonding between the PO_4^{3-} ion and the 6-membered ring in **3** (H-atoms not shown).

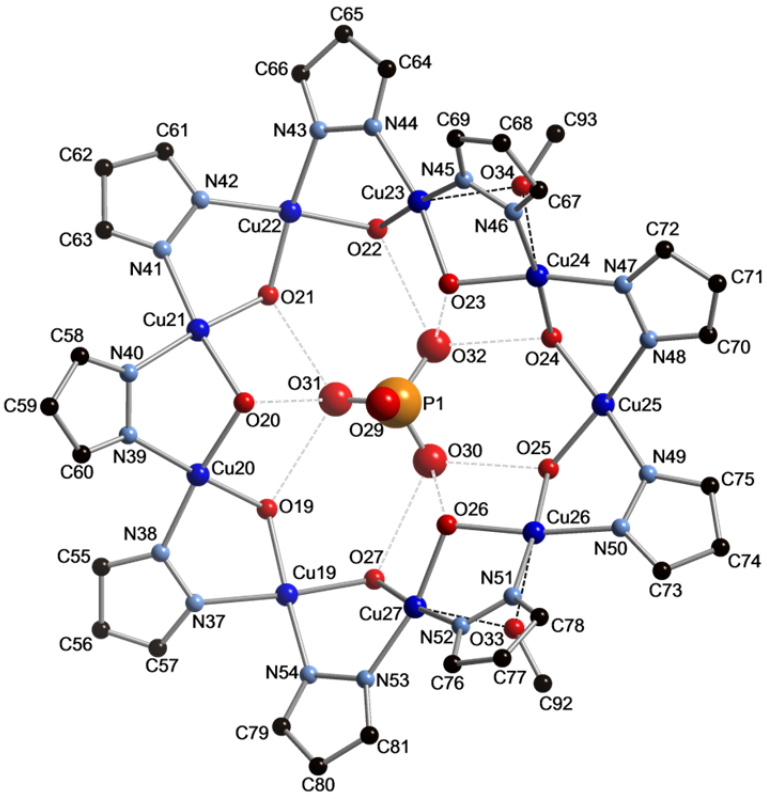

Figure S15. Hydrogen bonding between the PO_4^{3-} ion and the 9-membered ring in **3** (H-atoms not shown).

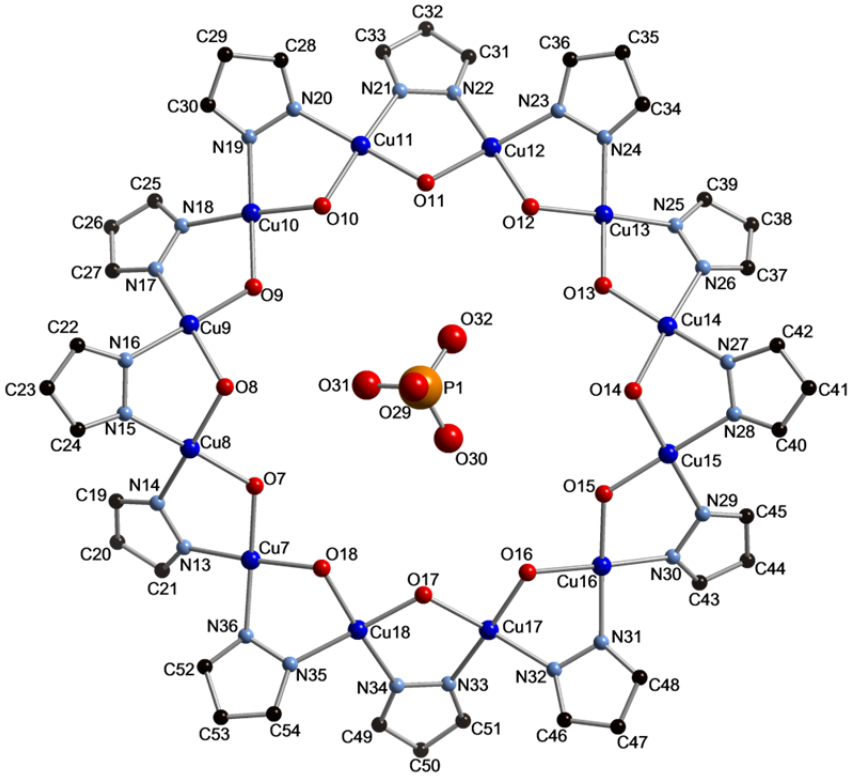

Figure S16. Illustration of the PO_4^{3-} ion centered above the 12-membered ring in **3** (H-atoms not shown).

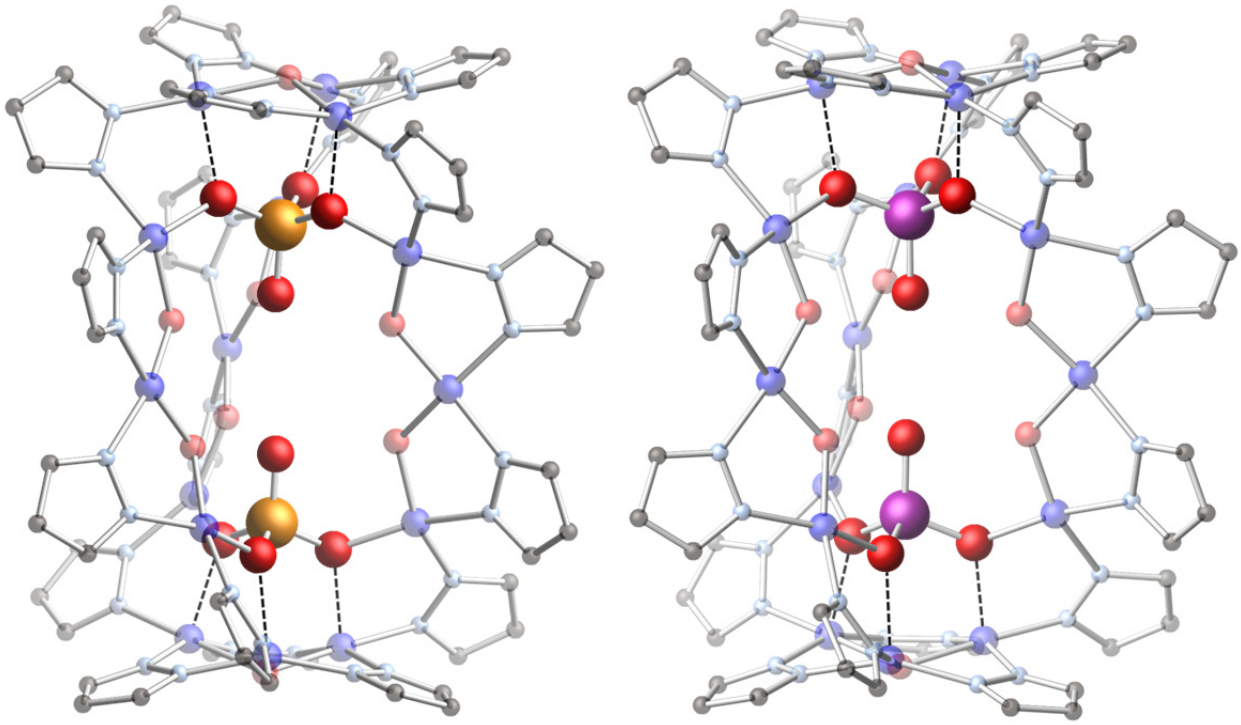

Figure S17. Comparative view of **4** (left) and **5** (right; only one of the two disordered molecules shown, see below), displaying the virtual identity of the two structures. In both cases, the M (Λ/Λ) enantiomer is shown. H-atoms are not shown for clarity. Color code: Cu−dark blue; P−orange; As−purple; O−red; N−light blue; C−black.

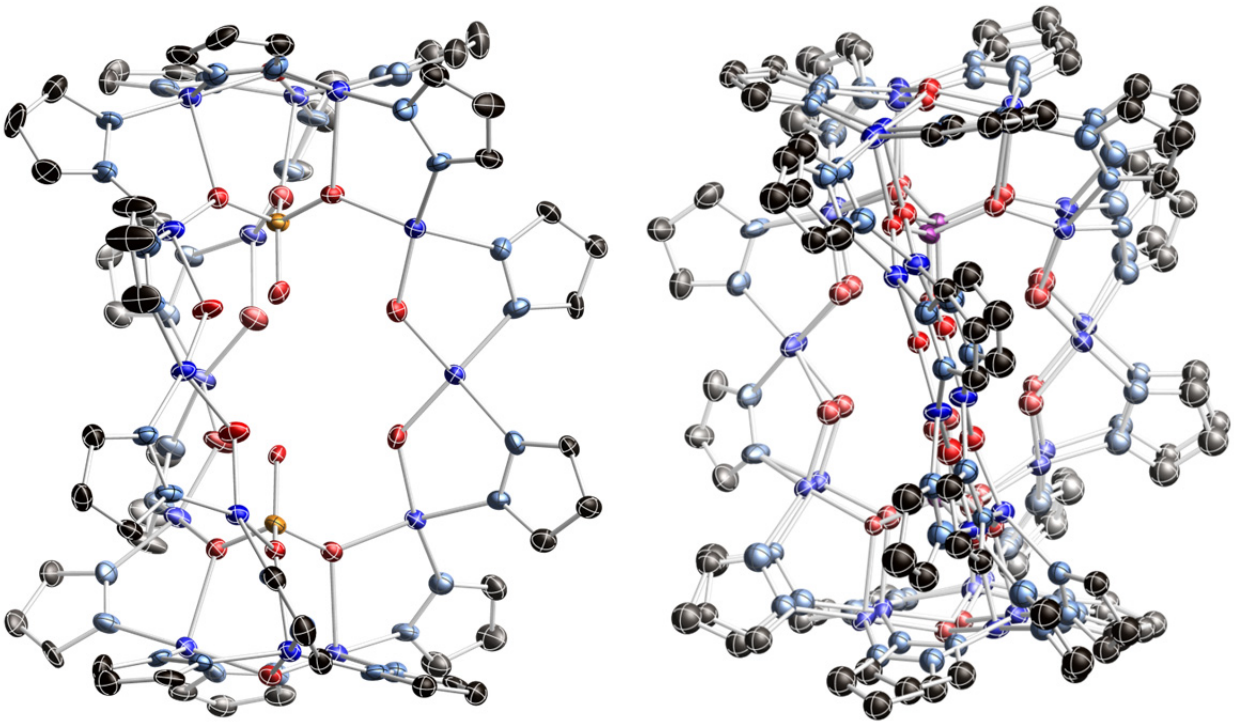

Figure S18. Thermal ellipsoid plots (50% probability) of **4** (left) and **5** (right, disordered). H-atoms, counterions and solvent molecules are omitted for clarity.

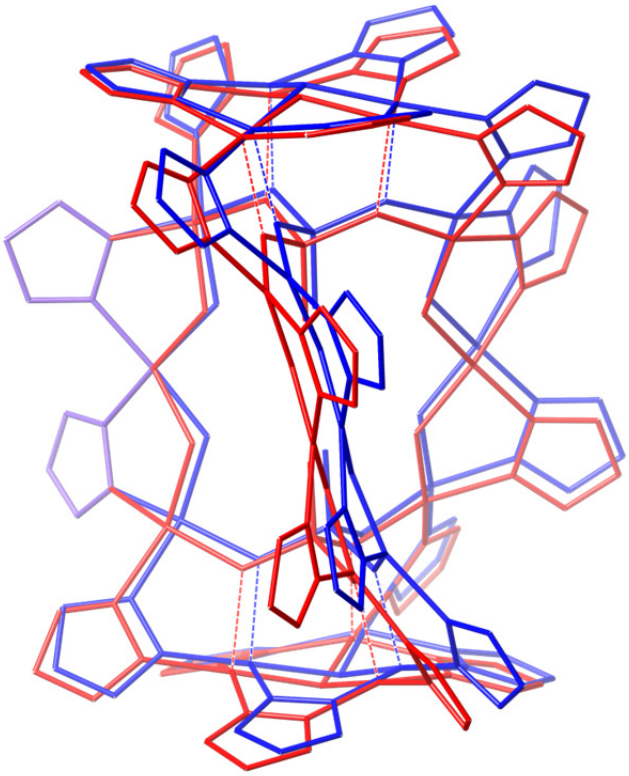

Figure S19. Illustration of the disorder in **5**. The two distinct components are shown in red and blue, respectively, and the shared $Cu(pz)_2$ unit is shown in violet.

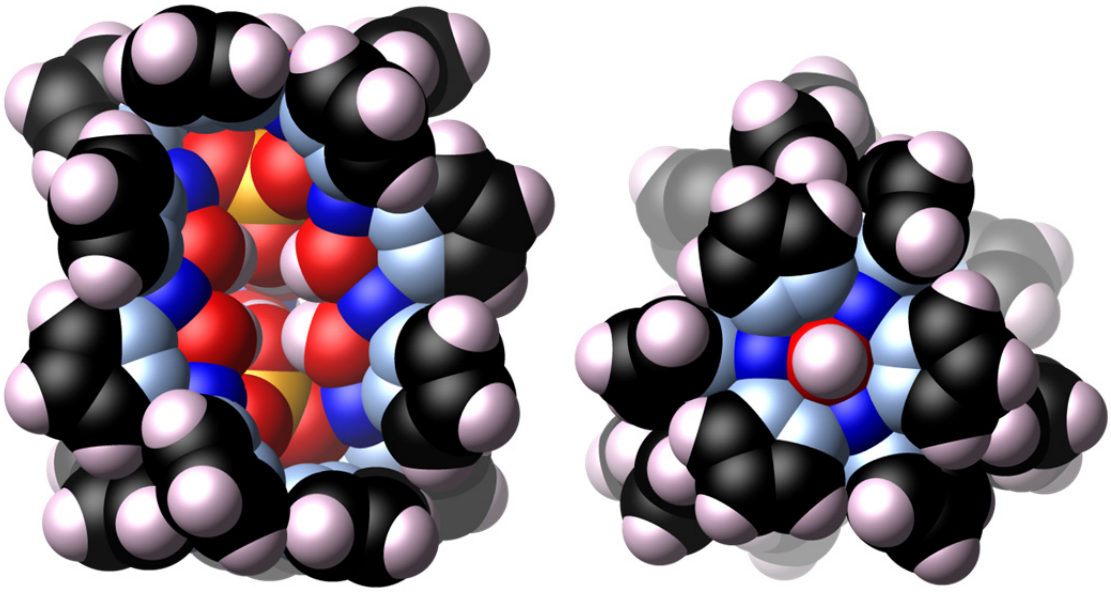

Figure S20. Space-filling representation (side- and top-views) of **4**. Color code: Cu−dark blue; P−orange; O−red; N−light blue; C−black; H−pink.

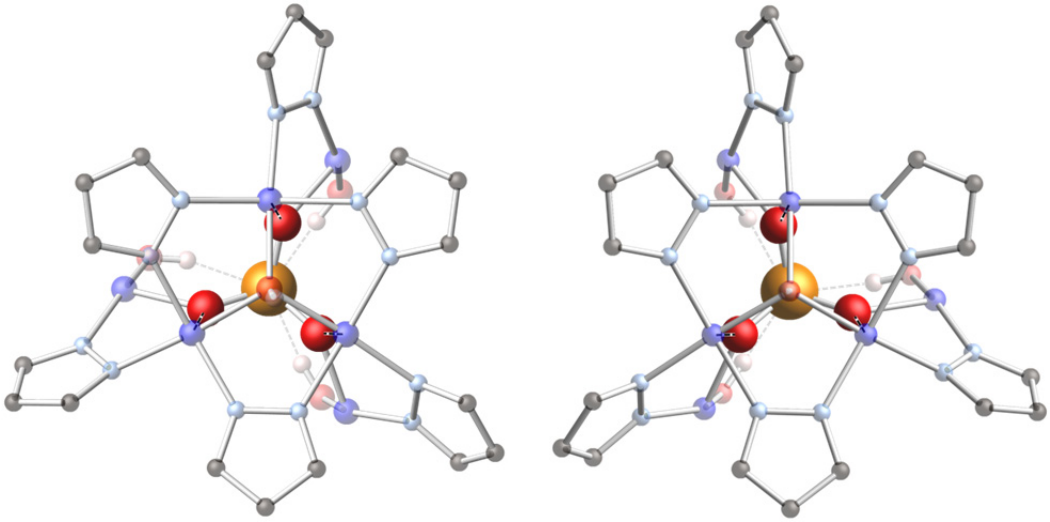

Figure S21. Clockwise (left) and counterclockwise (right) arrangement of the pyrazole moieties coordinated to the $Cu_3(\mu_3\text{-}OH)(\mu\text{-}pz)_3$ units, leading to chiral helicages **4** and **5** (partial structure of **4** is shown). Color code: Cu−dark blue; P−orange; O−red; N−light blue; C−black; H−pink (C−H hydrogens are not shown).